

Effect of recycled ratio on heat transfer performance of coal combustion in a 0.5MWth combustion test facility

A. A. Bhuiyan and J. Naser

Faculty of Science, Engineering and Technology (FSET)
 Swinburne University of Technology, VIC 3122, Australia.

Abstract

The power generation sector is facing an incessantly growing demand to reduce its emissions of CO₂. Oxy fuel combustion combined with CO₂ storage is suggested as one of the possible, promising technologies which will enable the continuous use of the burning coal or other fuels. This study presents a numerical investigation on performance of the combustion of Russian coal in a 0.5MWth small scale furnace. This finite volume based study is carried out using a commercial CFD code called AVL Fire version 2009.2. Devolatilisation and Char Combustion modelling are incorporated through user defined subroutines. For designing a new or retrofit an existing boiler for oxy fuel combustion capability, detailed study of heat transfer performance is important. This work is an attempt to model these issues and to address the effects of oxy-fuel firing on heat transfer performance. The main focus of this work is to determine the effect of recycled ratio (RR) on the flame heat transfer performance. The present numerical results are validated against the existing experimentally measured peak radiative heat flux and results showed reasonable agreement. In this study, four combustion environments were considered including an air-fired case (mainly N₂-based) as reference and three RR cases (mainly CO₂-based). Results were presented by temperature distributions and species distribution such as CO₂, H₂O, O₂ and H₂. From the results, it is found that the flames differed both in flame structure and scale for different cases. In air firing and RR75% cases, the flame is non-luminous, but at RR65% case, intense flame is observed. Also, the peak flame temperature profile moves upstream with the decrease of RR. A significant increase in the CO₂ concentrations were noted under all oxy-fuel combustion conditions compared to air-firing case.

Introduction

Combustion of coal results in the emission of greenhouse gases, the accumulation of which in the atmosphere since the start of the industrial revolution has been contributing to climate change which is responsible for the environmental and health threat. International efforts to mitigate the effect of climate change include Kyoto protocol and the establishment of an independent scientific advisory body and the intergovernmental panel on climate change which has accelerated efforts on the development of technologies to reduce carbon dioxide emission. For the reduction of CO₂ emissions from coal fired power plants, a number of CO₂ capture technologies, can be implemented for continuing the use of fossil fuel. Apart from these processes, different separation techniques are also suggested as gas phase separation, absorption, adsorption and hybrid processes. Recent developments in the CO₂ capture technologies include some innovative concepts (i.e. calcium looping, chemical looping, and amines scrubbing systems) suggested in literature. Based on carbon capturing system, oxy-fuel combustion is considered as a prominent technology for the abatement of CO₂ emission. Researchers have concentrated to the investigation and the development of oxy-fuel technology experimentally as well as

numerically in pilot/laboratory scale and industrial scale [1-7]. In this study, oxy-fuel concept is considered to investigate the effect of recycled ratio on heat transfer performance in different combustion environment using a commercial computational fluid dynamic code AVL Fire ver.2009.2. The main objective of this study is to examine the overall flame characteristics with the recycled ratios (RR) and associated combustion environment.

Furnace description and operating conditions

The 0.5MWth combustion test facility consists of 4m x 0.8m x 0.8m dimensions with 2.18m convergent section. The furnace is equipped by an aerodynamically air-staged burner for air-firing and oxy-firing cases. The detail of the burner design is given in [8-11]. In this study, Russian coal is considered as fuel. The proximate and ultimate analysis of the coal is given in table 1. In the experiment, initial start-up of the furnace is achieved by the combustion of the gas only until the flow parameters reached a steady state. The different operating conditions characterized by air-firing and three recycled ratio for oxy-firing cases. Different recycled ratios considered in this study are RR75%, RR72% and RR65%. The compositions of O₂ and CO₂ in different cases are presented in table 2. For all the cases, a constant primary flow was maintained at 15 m/s. In secondary flow, swirl is applied at a value of 0.6. The coal particle mass flow rate is 68 (kg/h) for all the cases simulated. The primary and secondary inlets were set at temperature of 343 K and 543 K respectively. No-slip boundary conditions were assumed and wall emissivity was set to 0.85 for the furnace wall. At exit of the furnace, zero gradient for all the variables are assumed. The different wall boundaries were characterized by thermal resistance as given in table 3. Coal particle distributions range of 75-300µm are considered in this study fitted with Rosin Rammler Distribution in CFD. More details about the coal particles are given in [8-10].

Proximate analysis, % ar		Ultimate analysis, % ar	
Volatile	33.55	Carbon	65.91
Ash content	11.98	Hydrogen	4.59
Fixed carbon	48.27	Nitrogen	2.09
Moisture	6.230	Sulphur	0.34
HHV, MJ/kg	27.098	Oxygen	8.89

Table 1. Properties of Russian coal

Case	Total flow, kg/h	O ₂ flow		CO ₂ flow	
		% ,mass	kg/h	% ,mass	kg/h
Air	745.7	23.3	--	--	--
RR75	757.1	21.0	159.0	79.0	598.1
RR72	669.6	23.4	156.7	76.6	512.9
RR65	523.0	29.3	153.3	70.7	369.7

Table 2. Boundary condition used [9-11]

Walls	Top	Bottom	Side	Quarl	Burner end
R, m ² K/W	0.397	0.235	0.109	0.109	0.109

Table 3. Thermal wall boundary conditions [12]

Mathematical models and numerical descriptions

In this study, 3D CFD simulation of coal combustion is carried out by a commercial CFD code, AVL Fire version.2009.2. Here, Eulerian/Lagrangian approach is considered for the modelling of fluid flow. Appropriate subroutines were written and coupled with the code for devolatilisation and char combustion. Regarding chemical reactions, three steps homogeneous reactions are considered for devolatilisation and one step heterogeneous reaction is considered for char oxidation modelling. To demonstrate the applications of combustion modelling in CFD, a detailed description of the used model is given in [1-7].

SIMPLE algorithm is used for the pressure velocity coupling. A general convergence criterion absolute residual value set to 10^{-4} for all the variables considered. Second order upwind scheme is considered for solving continuity equation. Particles are introduced in the furnace after achieving the quasi-steady state of all the parameters. For both gas and particle trajectories, 0.0025 (s) time step is used up to 40,000 time steps.

In order to achieve the level of confidence in the numerical result, three different grid sizes has been considered such as 500,000, 650,000 and 800,000 cells with similar meshing scheme in each cases. It was found that the mean temperature difference at a position of 0.3m from burner exit between 500,000-650,000 and 650,000-800,000 grid sets are found to be 1.43% and 0.7% respectively. Therefore, grid with 650,000 cells is considered with minimum computational time with reasonable accuracy in the present study.

In order to validate the model, available experimental [9] peak radiative heat flux is compared with the numerically predicted data. table 4 shows the comparison of the numerically calculated peak radiative heat flux with experimental data and a reasonable agreement has been observed for different cases. From the table, it is found that the variation of numerically calculated to the experimentally measured peak radiative heat flux is within the range of 5-10% in most cases.

Results and discussion

In this study, effect of recycled ratio on the overall heat transfer performance has been investigated considering different combustion environment. Results are presented based on temperature distribution, species distribution such as CO_2 , O_2 , H_2 , H_2O and hydrocarbon (CH_4) mass fraction etc. Radiative heat transfer performance is calculated on the furnace side wall. Table 4 indicates that radiative heat flux increases with the decrease of RR. It can be explained by the presence of oxidizer gas O_2 and CO_2 concentrations. With the increase of RR, O_2 concentration is decreasing. On the other hand Specific heat, C_p value of the flue gas increases because of the increase of CO_2 concentration. These observations are presented in figures 4 & 5. The combined effect of enriched oxidizing environment with reduced C_p is responsible for the decrease of peak radiative flux.

The axial velocity distribution along the radial direction at 0.3m from burner exit is presented in figure 1 for different cases. Flow variation is observed as mentioned in the flow boundary condition in table 2. At lower RR, mass flow is low. With the increase of RR, axial velocity (m/s) is high compared to other cases. This will provide less reaction time in the combustion area and comparatively lower flame temperature is expected.

Cases	Expt, KW/m^2	Pred, KW/m^2	Error,%
Air	390.00	431.58	10.6
RR75	340.00	393.46	15.7
RR72	370.00	398.29	7.65
RR65	495.00	522.71	5.60

Table 4. Comparison of peak radiative heat flux (KW/m^2)

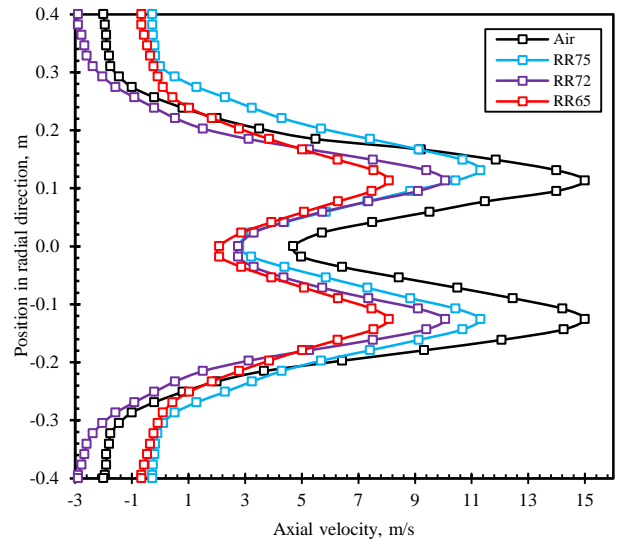


Figure 1. Axial velocity (m/s) distribution profile along the radial direction at 0.3m from burner end for different cases considered.

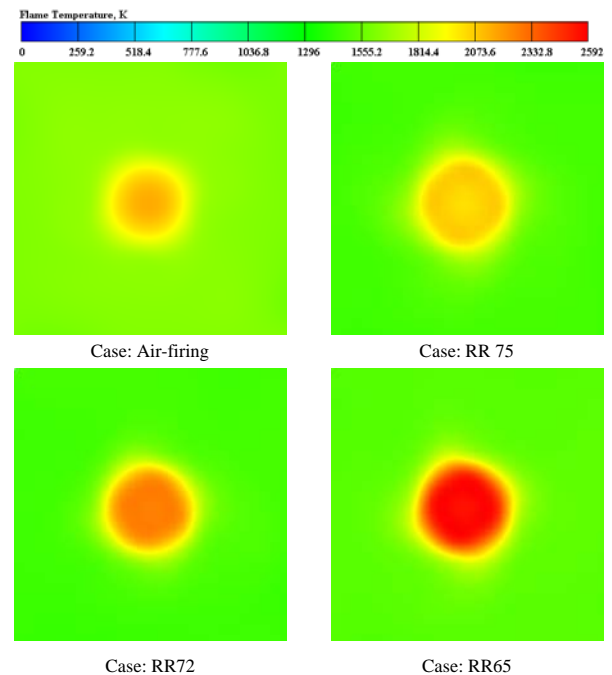


Figure 2. Flame temperature (K) distribution on the radial plane at a position of 0.3 m from the burner exit for four different cases considered.

The visualization of flame temperature distribution on the radial plane at a position 0.3m from the exit of the burner is presented for all the cases in figure 2. This position is chosen as most of the reaction occurred in this area. From these figure, it is found that the flames are more luminous and concentrated in the centre of the furnace in RR cases. But for air-firing case, flame is distributed. This variation can be described by the differences of the thermodynamic characteristics of N_2 and CO_2 . Comparatively brighter flame is observed in case of RR65 because of the low mass flow rate. The variation of flame temperature is also presented in figure 3 for different recycled cases compared with the reference air-firing case. It is found that the highest and lowest flame temperature is found in RR65 and RR75 cases respectively. But the trend of flame variation is identical in all the recycled cases. With the increase of RR, flame temperature profile goes downstream. This is due to quick combustion rate in oxidizer responsive environment in different recycled ratio cases.

Prediction of mass fraction (kg/kg) distribution of Carbon dioxide (CO_2) is important phenomena in oxy-fuel cases which contribute to the heat transfer, flame temperature characteristics. The CO_2 mass fraction (kg/kg) profile along the centre of the furnace for different cases is presented in figure 4. From the figure it is seen that in air-firing case, comparatively lower amount of CO_2 is experienced in combustion zone compared to oxy-fuel cases. With the increase of RR, CO_2 mass fraction is increased. Increasing the concentration of CO_2 in recycled cases has significant importance in combustion environment compared to air fired case. When CO_2 in the boiler decreases, the value of specific heat, C_p of the flue gas decreases. But the increase in oxidizer favours the combustion environment and increases the temperature, thus resulting in higher radiative heat transfer performance. The average value of CO_2 concentration for air-firing, RR75, RR72 and RR65 cases are found to be 0.17, 0.91, 0.90 and 0.85 respectively. Though the value of recycled ratio is increased, but the increase of CO_2 concentration is not significant. From this analysis, it can be concluded that if the generated CO_2 can be properly recycled and sequestered, a below-zero emission can be obtained.

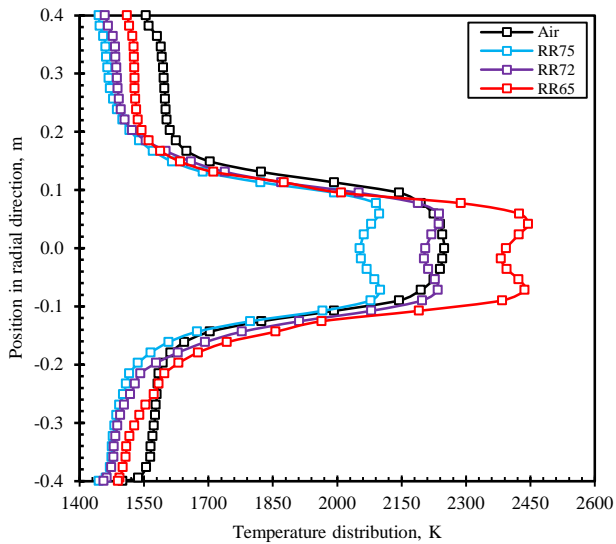


Figure 3. Flame temperature (K) distribution profile along the radial direction at 0.3m from burner end for different cases considered.

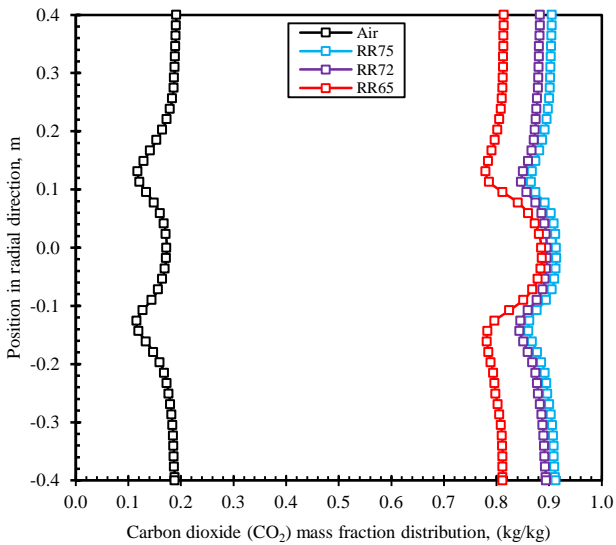


Figure 4. CO_2 mass fraction (kg/kg) distribution profile along the radial direction at 0.3m from burner end for different cases considered.

The Oxygen (O_2) mass fraction (kg/kg) distribution in the radial direction at a position of 0.3m from the burner exit for all the cases considered in this study is presented in figure 5. This type of profile is observed due to inlet boundary condition applied on the primary and the secondary annulus of the selected burner. In general, O_2 distribution is varied in different cases as shown in table 2. Due to swirl flow in the secondary annulus, peak of the O_2 concentration is seen in the same region for all the cases. But the central zone is almost O_2 free. When comparing to temperature profile in figure 3 with the O_2 concentration profile, there is a definite relation between these two. This phenomenon is in line with the fundamental described in literature. After devolatilisation, rest amount of O_2 is slowly reacted with the char particle. At lower RR, mass flow rate is low. So, char burns with the surrounding gases and increases the flame temperatures. When RR is decreasing resulting decrease in the volumetric flow, so that O_2 is distributed in more wide area as seen in the figure. But the peak O_2 concentration is found in similar area in the reaction zone for all the cases considered. When comparing to air firing case, peak O_2 concentration is almost similar in air firing and RR72 case.

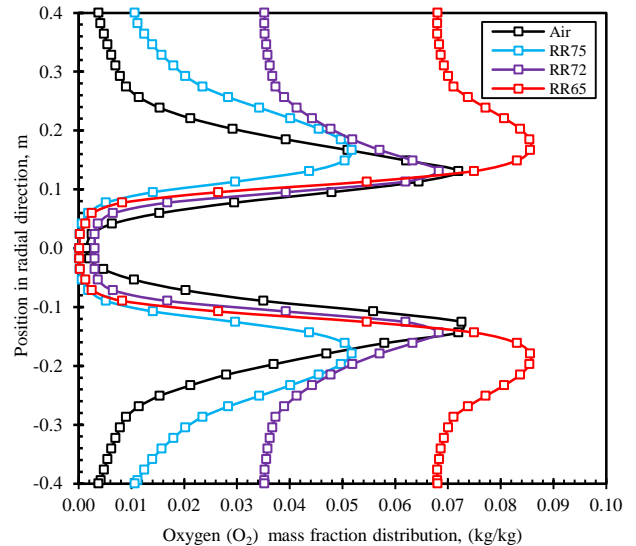


Figure 5. Oxygen (O_2) mass fraction distribution profile along the radial direction at 0.3m from burner end for different cases considered.

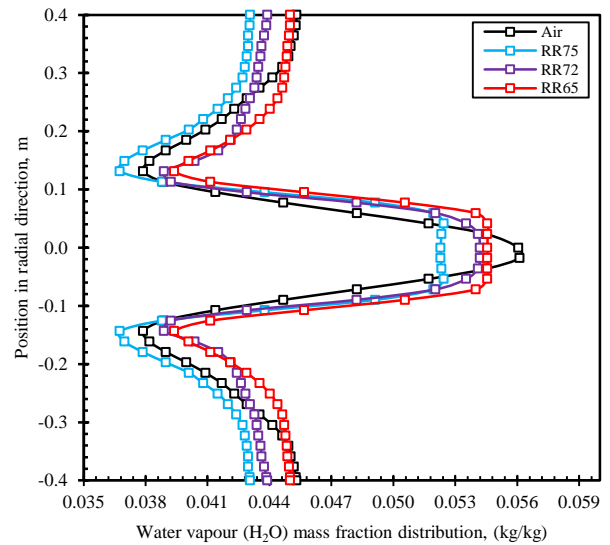


Figure 6. Water vapour (H_2O) mass fraction distribution profile along the radial direction at 0.3m from burner end for different cases considered.

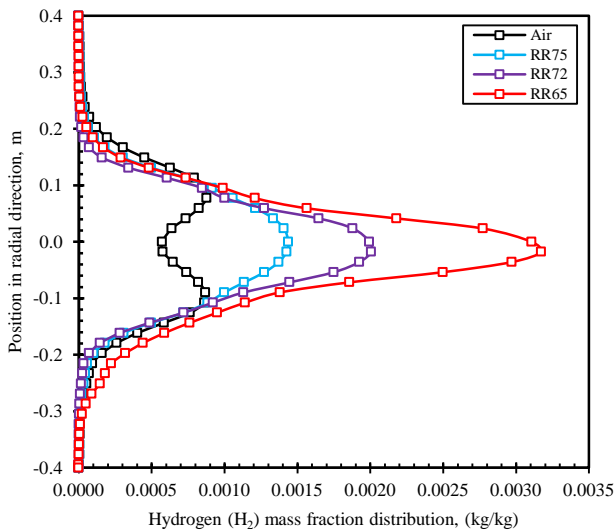


Figure 7. Hydrogen (H_2) mass fraction distribution profile along the radial direction at 0.3m from burner end for different cases considered.

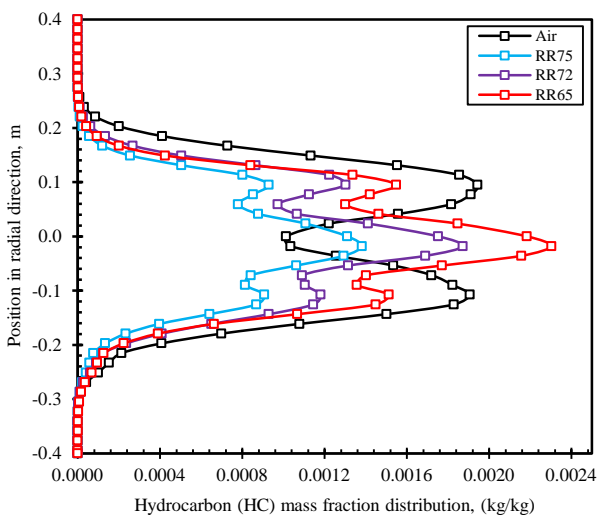


Figure 8. Hydrocarbon (CH_4) mass fraction distribution profile along the radial direction at 0.3m from burner end for different cases considered.

Figure 6 represents the water vapour mass fraction (kg/kg) distribution for the selected cases in this study. It is seen from the figure that highest value of the water fraction is found in the furnace centre. The particles are injected into the reaction zone of the furnace with the flow of primary oxidizer. So the peak value of the water vapour is found in this area. Another species, H_2 concentration (kg/kg) profile is presented in figure 7 for air-fired, RR75, RR72 and RR65 combustion scenarios. It is observed that H_2 concentration is higher for higher RR. For air-fired and RR75 case, lower prediction of H_2 is found. From the profile of H_2 mass fraction, it can be concluded that there is a definite relation between the formation of H_2 and the O_2 concentration shown in figure 5.

Figure 8 characterizes the mass fraction of hydrocarbon gas for all the cases considered. In this study, hydrocarbon gas is CH_4 equivalent because the product obtained from the homogeneous process of devolatilisation is similar to CH_4 . Figure indicates that higher mass fraction of hydrocarbon gas is found in the flame zone for the recycled cases. With the decrease of RR, CH_4 fraction is increased. This is because of the flow rate to the burner. With the decrease of RR, mass flow rate is decreased. This will provide the fuel to reside more in the reaction zone of the furnace which will increase the chance to release more hydrocarbon gas from the fuel particles.

Conclusions

A small scale CTF has been simulated by a CFD code coupled with the user-defined subroutines. This study presents the detailed combustion phenomena associated with the burning of coal under different cases. Simulation results were validated against the experimental data and the variation is in acceptable range. A detailed fundamental change in the main reaction zone inside the furnace for different recycled cases is investigated. Results are presented and explained based on the performance of the furnace and related productions from combustion reactions occurred. The variation of different combustion product such as CO_2 , H_2 , H_2O , O_2 and CH_4 mass fraction with the variation of recycled ratio is presented. The prediction suggested that with the increase of O_2 concentration in RR cases heat transfer and flame temperature improves significantly in RR72 and RR65 cases. It is also observed that air equivalent heat transfer and flame temperature can be attained in oxy-fuel cases.

References

- [1] Al-Abbas, A.H., Hart, J., and Naser, J., Numerical investigation of pyrolysis of a Loy Yang coal in a lab-scale furnace at elevated pressures, *Heat and Mass Transfer*, 2013. 49(12): p. 1725-1732.
- [2] Al-Abbas, A.H. and Naser, J., Numerical Modelling of Oxy-Fuel Combustion in a Full-Scale Tangentially-Fired Pulverised Coal Boiler, *Procedia Engineering*, 2013. 56: p. 375-380.
- [3] Al-Abbas, A.H. and Naser, J., Computational Fluid Dynamic Modelling of a 550 MW Tangentially-Fired Furnace under Different Operating Conditions, *Procedia Engineering*, 2013. 56: p. 387-392.
- [4] Al-Abbas, A.H., Naser, J. and Dodds, D., CFD modelling of air-fired and oxy-fuel combustion in a large-scale furnace at Loy Yang A brown coal power station, *Fuel*, 2012. 102: p. 646-665.
- [5] Al-Abbas, A.H. and Naser, J., Numerical study of one air-fired and two oxy-fuel combustion cases of propane in a 100 kW furnace, *Energy & Fuels*, 2012. 26(2): p. 952-967.
- [6] Al-Abbas, A.H. and Naser, J., Effect of chemical reaction mechanisms and NO x modeling on air-fired and oxy-fuel combustion of lignite in a 100-kW furnace, *Energy & Fuels*, 2012. 26(6): p. 3329-3348.
- [7] Al-Abbas, A.H., Naser, J. and D. Dodds, CFD modelling of air-fired and oxy-fuel combustion of lignite in a 100KW furnace, *Fuel*, 2011. 90(5): p. 1778-1795.
- [8] Bhuiyan, A.A. and Naser, J., Numerical modelling of oxy fuel combustion, the effect of radiative and convective heat transfer and burnout. *Fuel*, 2014.
- [9] Smart, J.P., Patel, R. and Riley, G.S., Oxy-fuel combustion of coal and biomass, the effect on radiative and convective heat transfer and burnout, *Combustion and Flame*, 2010, 157(12): p. 2230-2240.
- [10] Smart, J.P., O'Nions, P. and Riley, G.S., Radiation and convective heat transfer, and burnout in oxy-coal combustion, *Fuel*, 2010. 89(9): p. 2468-2476.
- [11] Smart, J.P., Lu, G., Yan, Y. and Riley, G.S., Characterisation of an oxy-coal flame through digital imaging, *Combustion and Flame*, 2010. 157(6): p. 1132-1139.
- [12] Stechly, K.S., Wechel, G., and Ingham, D., CFD modelling of air and oxy-coal combustion, *Int. Journal of Numerical Methods for Heat & Fluid Flow*, 2014. 24(4): p. 5-5.